Geology

Schwertmannite in wet, acid, and oxic microenvironments beneath polar and polythermal glaciers

R. Raiswell, L.G. Benning, L. Davidson, M. Tranter and S. Tulaczyk

E-mail alerting services	click www.gsapubs.org/cgi/alerts to receive free e-mail alerts when new articles cite this article
Subscribe	click www.gsapubs.org/subscriptions/index.ac.dtl to subscribe to Geology
Permission request	click http://www.geosociety.org/pubs/copyrt.htm#gsa to contact GSA

Notes

THE
GEOLOGICAL
SOCIETY
OF AMERICA

Schwertmannite in wet, acid, and oxic microenvironments beneath polar and polythermal glaciers

R. Raiswell[1]*, L.G. Benning[1], L. Davidson[1], M. Tranter[2], and S. Tulaczyk[3]
[1]Earth and Biosphere Institute, School of Earth and Environment, Leeds University, Leeds LS2 9JT, UK
[2]Bristol Glaciology Centre, School of Geographical Sciences, Bristol University, Bristol BS8 1SS, UK
[3]Department of Earth and Planetary Sciences, University of California–Santa Cruz, Santa Cruz, California 95064, USA

ABSTRACT

Glacial and iceberg sediments contain nanoparticulates of schwertmannite, ferrihydrite, and goethite formed where pyrite was oxidized by dissolved oxygen in aqueous subglacial environments. Schwertmannite, typically found in acid mine drainage, only forms at low pH by the oxidative weathering of pyrite. Stoichiometric models show that these conditions can be created in closed-system microenvironments containing at least 10^{-4} M dissolved oxygen, where volume ratios of water/pyrite are ~10^5 to 10^6. Ferrihydrite is the only product at higher and lower volume ratios. In these microenvironments the oxidation of pyrite to form schwertmannite is possible in several decades. Schwertmannite and ferrihydrite are metastable in contact with water and are transformed to goethite in <100 yr unless preserved in ice. The presence of these nanoparticulates demonstrates the existence of transient, acidic, and oxic aqueous microenvironments where enhanced biochemical and/or geochemical activity occurs beneath glaciers and ice sheets.

INTRODUCTION

The subglacial biosphere is currently of interest as a potential analogue for extraterrestrial microbial life. However, biochemical and/or geochemical conditions in subglacial environments can only be inferred from measurements of meltwaters sampled from glacial outlets or drillholes reaching the ice-rock interface (Tranter et al., 1997). These subglacial waters integrate chemical signals from a relatively large area and cannot demonstrate small-scale spatial and temporal variability. By contrast, authigenic minerals in subglacial sediments can preserve a remnant signal from transient, biochemically and geochemically active subglacial microenvironments.

Raiswell et al. (2006, 2008) have shown that subglacial sediments contain authigenic ferrihydrite and goethite as nanoparticulates. Here we present further chemical and microscopic data of Fe-bearing nanoparticulates in sediments from icebergs and basal glacier ice from Antarctica and Svalbard, and show that these nanoparticulates provide a mineral signature for hotspots of biochemical and/or geochemical activity in the subglacial environment.

SAMPLING AND METHODOLOGY

Chemical and microscopy studies were carried out on the following samples (described by Raiswell et al., 2008); icebergs S1–S4 from the Weddell Sea (Antarctica), icebergs KG1–KG2 collected from Admiralty Strait (Southern Ocean), plus basal ice from Taylor Glacier (T1–T3) and Canada Glacier (C1) in the Dry Valleys (Antarctica). All the iceberg samples were collected from sediment-bearing layers in dense, clear blue ice representing compressed glacier ice (Raiswell et al., 2008). The Taylor and Canada samples were derived from slabs of basal sediment-bearing ice low in solutes (e.g., Fe and Cl; Raiswell et al., 2008). In addition, two new samples were collected from sediment-rich (SV1) and sediment-poor (SV2) basal ice in Monaco Glacier (Svalbard, 79°30′N, 12°40′E), and three new samples (IS2B, IS3B, and IS3T) were collected from water-saturated sedi-

ments at the base of the West Antarctic Ice Stream (82°22′S, 136°24′W). Sediment samples were treated by an ascorbate solution, which extracts fresh, nanoparticulate ferrihydrite (Hyacinthe and Van Cappellen, 2004) and partially extracts schwertmannite (see the GSA Data Repository[1]). The Fe removed by ascorbate is hereafter termed FeA. The residual sediment was extracted with sodium dithionite (Raiswell et al., 1994), which removes Fe present as residual, aged ferrihydrite plus goethite, hematite, and lepidocrocite (termed FeD). High-resolution imaging, nanodiffraction, and elemental analysis of the sediments was carried out using a field emission gun—transmission electron microscope (FEG-TEM) equipped with an energy dispersive X-ray spectrometer (EDS) and selected area electron diffraction (SAED) capabilities (see the Data Repository).

RESULTS

Figure 1 shows typical occurrences of Fe-bearing nanoparticulates with their X-ray diffraction (XRD) patterns and elemental compositions. As-rich schwertmannite was identified in samples from the Taylor, Canada, and Monaco Glaciers by the characteristic stumped pin-cushion morphology, XRD lines at 2.55 and 1.51 Å, and EDS analysis (which shows an Fe-, S-, and As-rich composition; see Figs. 1A, DR1, and DR2). Ferrihydrite occurs as nanoparticles (5–10 nm diameter) in structureless aggregates, which have an XRD pattern similar to that of schwertmannite, but do not show the distinctive pin-cushion morphology (Fig. 1B). EDS analysis of ferrihydrite confirms an Fe-rich composition with S and As absent. Goethite was identified by its morphology and characteristic XRD lines (i.e., 4.18, 2.69, 2.45, 1.72, and 1.56 Å), and was found as laths typically <100 nm in length and 5–10 nm in diameter, which were often assembled into bundles (Fig. 1C). Goethite also occurred in aggregates in which adjacent nanoparticles were ordered, as shown by a crude alignment of their lattice fringes (Fig. 1C). The ice stream samples contained unidentified Fe-bearing nanoparticulates rich in Ti and Si. The %FeA and %FeD extraction data are shown in Table DR1.

INTERPRETATION

Origin of Fe Nanophases

Nanoparticulates of schwertmannite, ferrihydrite, and goethite are believed to form at high degrees of supersaturation (Waychunas et al., 2005) that could result from repeated freezing and melting cycles (Raiswell et al., 2008). It is unlikely that these phases were present prior to glacial weathering because nanoparticles are metastable, and do not survive over geological time scales (see following). Instead these Fe-bearing nanoparticles form by chemical weathering of pyrite in subglacial sediment where water is present. Pyrite oxidation initially produces Fe^{2+}, which is hydrolyzed to octahedral $Fe^{3+}(O, OH, OH_2)$ units that slowly aggregate to colloi-

[1]GSA Data Repository item 2009107, details of the analytical methodology, analyses of %FeA and %FeD (in samples plus synthetic and natural iron minerals), and high-resolution TEM, SAED, and EDS data for samples from the Canada and Monaco Glaciers is available online at www.geosociety.org/pubs/ ft2009.htm, or on request from editing@geosociety.org or Documents Secretary, GSA, P.O. Box 9140, Boulder, CO 80301, USA.
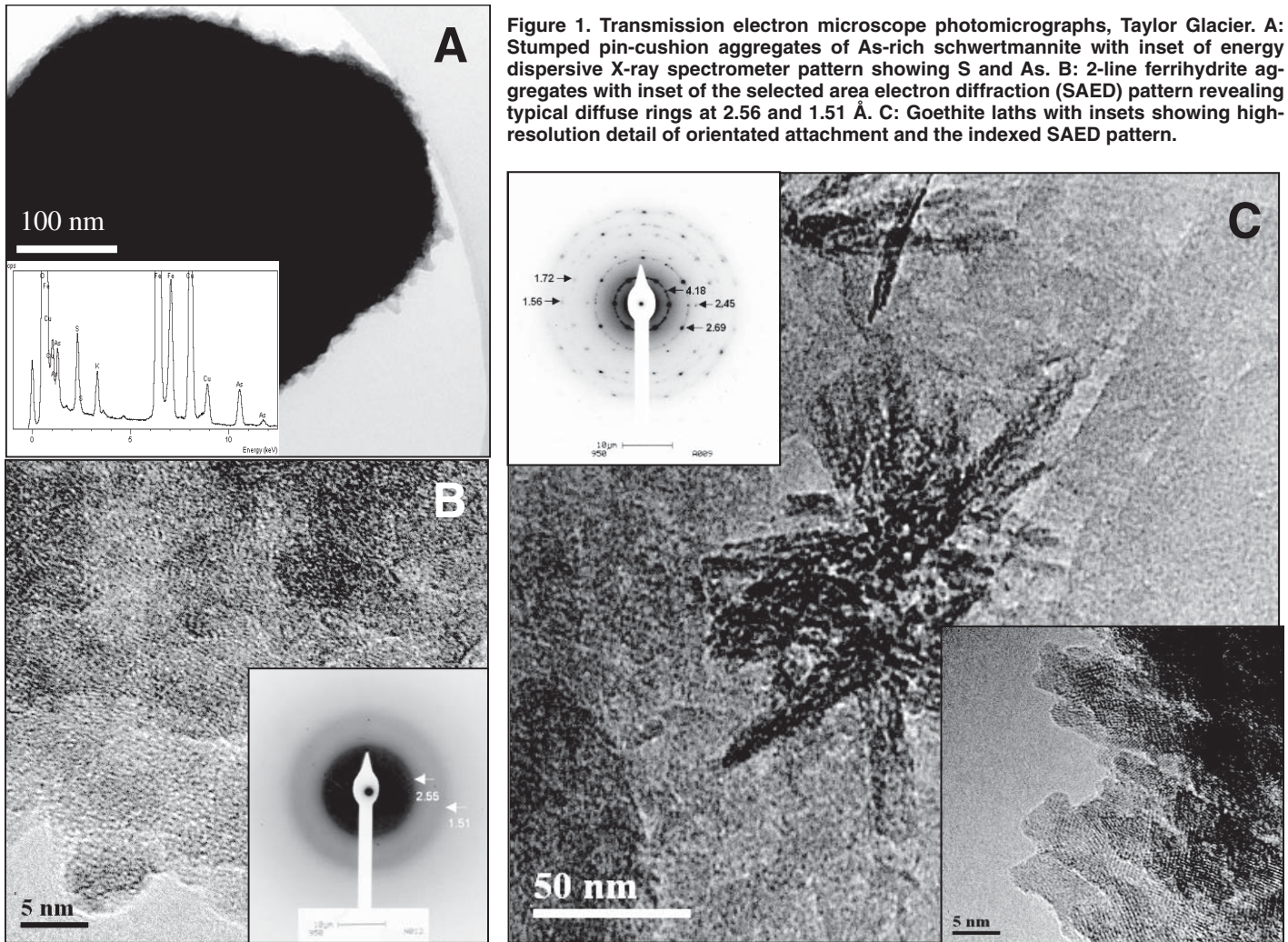
Figure 1. Transmission electron microscope photomicrographs, Taylor Glacier. A: Stumped pin-cushion aggregates of As-rich schwertmannite with inset of energy dispersive X-ray spectrometer pattern showing S and As. B: 2-line ferrihydrite aggregates with inset of the selected area electron diffraction (SAED) pattern revealing typical diffuse rings at 2.56 and 1.51 Å. C: Goethite laths with insets showing high-resolution detail of orientated attachment and the indexed SAED pattern.

dal sizes. Green rust could be a possible intermediate (Ruby et al., 2006), but requires fully anaerobic conditions and a higher pH than schwertmannite. These nanoparticulates are metastable, but persist in nature where the transformation kinetics are slow (see Waychunas et al., 2005).

The %FeA and %FeD data (Table DR1) are consistent with our samples comprising schwertmannite and fresh 2 line ferrihydrite, along with dithionite-soluble phases (goethite, 6 line ferrihydrite). Schwertmannite is a poorly ordered ferric oxyhydroxy-sulfate or nanophase with a compositional range of $Fe_3O_8 (OH)_{8-2x} (SO_4^{2-})_x \cdot nH_2O$, where $x = 1–1.75$ and $n = 8.17–8.62$ (Yu et al., 2002). Schwertmannite only forms by the oxidative weathering of pyrite at pH 2–5, and ferrihydrite is the main product at near-neutral pH (Bigham et al., 1996). Arsenic (as the arsenate ion) substitutes for sulfate and is a common trace component of schwertmannite found in acid mine drainage. At low As/(As + Fe) ratios, the classic pin-cushion morphology is retained, but the needles are progressively blunted (Fig. 1A) with increasing As content (Carlson et al., 2002). Schwertmannite transforms via a ferrihydrite intermediate to goethite or hematite (Davidson et al., 2008). Figure 1C shows that goethite nanoparticles aggregate by orientated attachment, which occurs where Brownian motion collisions between nanoparticles align their lattice fringes (Banfield et al., 2000).

The occurrence of schwertmannite clearly demonstrates the presence of subglacial environments where aqueous, oxidative weathering of pyrite occurs. These environments must typically have high enough dissolved concentrations of Fe^{3+} to precipitate ferrihydrite at near-neutral pH, with schwertmannite forming in hotspots having (SO_4^{2-}), pH 2–5, and higher

(Fe^{3+}). Schwertmannite, ferrihydrite, and goethite all require water for their formation (Schwertmann and Murad, 1983; Davidson et al., 2008), and their presence demonstrates the existence of subglacial water. Regelation induces melting and refreezing at bedrock obstructions in the polythermal Monaco Glacier, and bedrock temperatures allow water to be abundant. However, temperatures in the Taylor and Canada Glaciers are too low ($<–10\ °C$) for water to be abundant, although zones of temperate ice may exist (Hubbard et al., 2004). Water may also occur as a thin film (20–40 nm thick) at the ice-rock interface of these glaciers (Cuffey et al., 1999).

Stoichiometric Models of Schwertmannite and Ferrihydrite Formation

Further insight into the conditions that produce schwertmannite can be gained by stoichiometric modeling. Pyrite is the most likely mineral reactant (Tranter et al., 1993). However, oxidation can occur aerobically and anaerobically (Williamson and Rimstidt, 1994) using either dissolved O_2, NO_3^-, or Fe^{3+}. Dissolved O_2 is often depleted in glacial meltwaters by pyrite oxidation (Tranter et al., 1993). Nitrate depletion also occurs but concentrations are low in meltwaters (Bottrell and Tranter, 2002), and O_2 must first be consumed in order to establish the suboxic conditions required for NO_3^- reduction. The stoichiometry of pyrite oxidation by dissolved O_2 and Fe^{3+} (Williamson and Rimstidt, 1994) is compared here:

$$2FeS_2 + 15/2O_2 + H_2O \rightarrow 4SO_4^{2-} + 2Fe(OH)_3 + 8H^+, \qquad (1)$$

$$FeS_2 + 14Fe^{3+} + 8H_2O \rightarrow 2SO_4^{2-} + 15Fe^{2+} + 16H^+. \qquad (2)$$
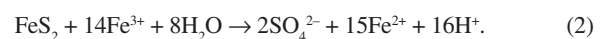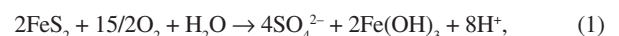
Concentrations of Fe^{3+} in our glacial ice are <4 nM (Raiswell et al., 2008), which can oxidize only trivial amounts of pyrite anaerobically. Aerobic oxidation using Fe^{3+} is possible because oxygen is present to reoxidize Fe^{2+} to Fe^{3+}:

$$2Fe^{2+} + 1/2O_2 + 5H_2O \rightarrow 2Fe(OH)_3 + 4H^+. \qquad (3)$$
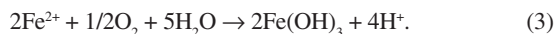
However, the oxidation of pyrite by Fe^{3+} in Equations 2 and 3 consumes exactly the same amount of dissolved O_2 as in Equation 1.

Hence the stoichiometric model is based on Equation 1 for pyrite oxidation in 1 L of pure water (pH 7) using dissolved O_2. The model assumes that there are no additions of O_2 or losses of solutes from outside the system. The solubility product of ferrihydrite (log K_{so} = −39; Cornell and Schwertmann, 2003) is so low that only trivial amounts of Fe^{3+} are required to reach saturation at pH 6–7, and thus the Fe^{3+} concentration is controlled by ferrihydrite saturation until increasing concentrations of Fe^{3+}, SO_4^{2-}, and H^+ produce schwertmannite saturation (log K_{so} = −18 ± 2.5; Bigham et al., 1996).

Figure 2 shows the model changes in the concentrations of SO_4^{2-}, H^+, and Fe^{3+} (in equilibrium with schwertmannite and/or ferrihydrite) and the ion activity product of schwertmannite (IAP_{sch}) as a function of O_2 consumed. Concentrations of SO_4^{2-} and H^+ increase during the early stages of reaction, but ferrihydrite saturation is maintained because Fe^{3+} concentrations increase more rapidly than OH^- concentrations decrease (Fig. 2). These changes also increase the IAP_{sch}, which exceeds the solubility product (making schwertmannite more stable than ferrihydrite) once ~10^{-4} mol of O_2 have been consumed. The model is insensitive to starting pH values, and an initial pH of 5 (instead of 7) only decreases the pH by 0.2 when 10^{-4} mol of O_2 are consumed.

This model also places constraints on the size of the oxidizing environment, assuming 1 mol of pyrite requires 3.75 mol of O_2 for complete oxidation and dissolved O_2 is 1–4.5 × 10^{-4} M (ranging from the lowest concentration producing schwertmannite saturation up to equilibrium concentrations at 0 °C; Benson and Krause, 1980). Thus 1 mol of pyrite requires 9–36 m^3 of meltwater for complete oxidation. A pyrite grain of radius r (m) and density d (5 × 10^6 g m^{-3}) contains 0.17 × 10^6 r^3 mol of pyrite and so needs (1.5–6) × 10^6 r^3 m^3 of oxygenated water. The volume ratio (water)/ (pyrite) = (0.3–1.5) × 10^6, which occurs when a grain of 1 μm radius is in contact with a thin film of oxygenated water 30 nm in height and ~7–14 mm long and wide. These volume estimates indicate that oxidative subglacial weathering is confined to microenvironments. Subglacial microenvironments with volume ratios smaller 0.3 × 10^6 contain insufficient O_2 to oxidize enough pyrite to form schwertmannite. Volume ratios >1.5 × 10^6 contain insufficient pyrite to accumulate high enough concentrations of dissolved products to reach schwertmannite saturation. Ferrihydrite is the only product at these lower and higher volume ratios. Note that the volume ratios would increase by a factor of 2 if the microenvironment was water-saturated sediment with a porosity of 50%. Schwertmannite formation only occurs at pH < 5, but the dissolution of carbonate may buffer pH values to higher values (>5.5) that prevent schwertmannite formation.

Rates of Pyrite Oxidation

Empirical rate laws (Williamson and Rimstidt, 1994) permit a rough estimate of the time needed to oxidize pyrite by dissolved O_2:

$$\text{rate of pyrite oxidation, (mol}^2 \text{ m}^{-2} \text{ s}^{-1}) = 10^{-8.19} (O_2)^{0.5}/(H^+)^{0.11}, \qquad (4)$$

where (O_2) is the concentration of dissolved oxygen and (H^+) is the activity of H^+. Schwertmannite saturation is reached after the consumption of ~10^{-4} mol of O_2 and, at this point in the reaction (indicated by star in Fig. 2), (Fe^{3+}) = $10^{-8.72}$ and the residual (O_2) ranges from 1 to 3.5 × 10^{-4} M, and pyrite is being oxidized at a rate of (2–4) × 10^{-10} mol m^{-2} s^{-1} (from Equation 4). An
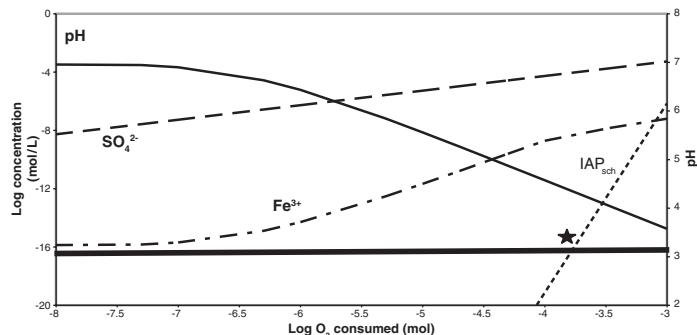
Figure 2. Stoichiometric model of closed-system oxidation of pyrite by dissolved oxygen in glacial meltwaters. Concentrations of Fe^{3+} (dots and dashes) represent equilibrium with ferrihydrite. Dotted line shows ion activity product (IAP) of schwertmannite, which reaches saturation levels above horizontal shaded line.

idealized spherical pyrite grain of radius (r) contains 0.17 × 10^6 r^3 moles of pyrite, has a surface area of 1.4 × 10^4 r mol m^{-2}, and can be oxidized in (1.4 × 10^4 r)/[(2 – 4) × 10^{-10} × 3.15 × 10^7] yr. A 1-μm-radius pyrite grain would fully oxidize in ~1–2 yr and a 10 μm grain in ~10–20 yr. Up to the point of schwertmannite saturation these rates are faster than those estimated by the Williamson and Rimstidt (1994) equations for oxidation using Fe^{3+} at the trace concentrations shown in Figure 2, and faster than those for microbial oxidation in the presence of O_2 (Gleisner et al., 2006).

These estimates are only approximate for several reasons. First, rates are derived for room temperature and may be an order of magnitude slower at subglacial temperatures. Second, rates have been estimated using a constant surface area. Third, rates may be enhanced by microbial involvement (Sharp et al., 1999) where there are optimal conditions of low pH and high (Fe^{3+}) and (O_2) (Gleisner et al., 2006). Overall it is clear that schwertmannite may form in less than several decades in subglacial environments by pyrite weathering, even without involving microbial activity (which may further enhance oxidation rates).

Transformation of Schwertmannite and Ferrihydrite

Studies of the transformation of schwertmannite to goethite can be used to estimate the half-life for the survival of schwertmannite in glacial environments. Davidson et al. (2008) studied the transformation of schwertmannite to goethite at pH 13.2 and temperatures from 60 to 190 °C. An Arrhenius plot of their rate constant data versus reciprocal temperature has the form:

$$\ln (k) = -3973 (1/T) + 3.18, \qquad (5)$$

(r = 0.97) where k is the rate constant and T is temperature (in K). Equation 5 can be used to estimate the effects of temperature and the ratio of the rate constants at 0 °C (k_0) and 25 °C (k_{25}), given by:

$$\ln (k_0)/\ln (k_{25}) = 1.12. \qquad (6)$$

A rough estimate of the rate constants for this transformation at pH 6 and 7.2 and 25 °C can be made from the data of Schwertmann and Carlson (2005), which show an approximate first-order relationship for the production of H^+ during the transformation of schwertmannite to goethite. The first-order rate constants at 25 °C are 0.0038 and 0.0024 day^{-1} at pH 7.2 and 6, respectively, or 0.0018 and 0.0012 day^{-1} at 0 °C (from Equation 6). Thus schwertmannite in contact with water at 0 °C and pH 6–7.2 has a half-life of 1–2 yr.

Ferrihydrite in our samples may represent an intermediate formed as schwertmannite transforms to goethite or hematite (Davidson et al., 2008),

or may be formed directly from the breakdown of pyrite. The transformation of ferrihydrite to goethite proceeds by a dissolution-reprecipitation mechanism, the rate of which is limited by the solubility of ferrihydrite (Yee et al., 2006). Conversion to hematite is favored at pH 6–8, where the solubility of ferrihydrite is low and appears to occur by orientated attachment (Fig. 1C). Schwertmann and Murad (1983) gave half-lives for the conversion of ferrihydrite to goethite-hematite mixtures at pH 6 (166 days) and pH 7 (112 days) at 24 °C. Decreasing temperature decreases the rate of transformation, which may take several years at 4 °C (Cornell and Schwertmann, 2003).

These kinetic data are for pure phases (and should be interpreted cautiously), but the passage of 3 half-lives results in a 95% transformation, and it seems unlikely that either schwertmannite or ferrihydrite could survive for >100 yr in contact with water, unless stabilized by the coprecipitation of transition metals or oxyanions (e.g., Davidson et al., 2008). The presence of these Fe-rich nanophases therefore indicates the transient nature of the oxidative weathering microenvironments, and their long-term survival requires that contact with water is prevented by freezing into ice.

CONCLUSIONS

Nanoparticulate schwertmannite occurs in ice-hosted sediments from Arctic and Antarctic glaciers, and nanoparticulate ferrihydrite and goethite occur in icebergs from Antarctica. The presence of schwertmannite indicates the occurrence of oxidative, subglacial weathering of pyrite at low pH (2–5), and does not necessarily involve microbial activity. Stoichiometric modeling shows that schwertmannite occurs where pyrite is oxidized by dissolved O_2 in a closed system, after the consumption of $\sim 10^{-4}$ mol of dissolved O_2 (corresponding to a microenvironment with a water/pyrite volume ratio of $\sim 10^5$). Microenvironments with smaller volume ratios may contain insufficient dissolved O_2 to reach schwertmannite saturation, and larger volume ratios ($>\sim 10^6$) produce fluids that are too dilute to reach schwertmannite saturation. In both cases pyrite weathering will only produce ferrihydrite.

Estimates of the rate of pyrite oxidation by dissolved O_2 indicate that several decades are needed for the oxidation of pyrite grains (r < 10 μm) in closed-system microenvironments. Furthermore, the transformations of schwertmannite to goethite, and ferrihydrite to goethite, in contact with water require <100 yr. Longer-term survival of schwertmannite and ferrihydrite thus requires isolation from water by freezing.

The presence of nanoparticulate schwertmannite clearly indicates the existence of transient, aqueous subglacial microenvironments. These exist in polythermal glaciers, where regelation induces melting and refreezing at bedrock obstructions and where bedrock temperatures allow water to be abundant. However, in polar glaciers such as the Taylor and Canada Glaciers, temperatures are <−10 °C, and the glaciers move too slowly to permit regelation; however, transient aqueous microenvironments may exist in zones of temperate ice or in thin films of water at the ice-rock interface. The formation, preservation, and delivery of nanoparticulate schwertmannite and ferrihydrite into the Southern Ocean may exert an important influence on the Fe biochemical-geochemical cycle by relieving Fe-limited productivity and so stimulating present productivity and productivity during the Last Glacial Maximum (Raiswell et al., 2008).

REFERENCES CITED

Banfield, J.F., Welch, S.A., Zhang, H., Ebert, T.T., and Penn, R.L., 2000, Aggregation-based crystal growth and microstructure development in natural iron oxyhydroxide biomineralisation products: Science, v. 289, p. 751–754, doi: 10.1126/science.289.5480.751.

Benson, B.B., and Krause, D.K., Jr., 1980, The concentration and isotopic fractionation of gases dissolved in freshwater in equilibrium with the atmosphere. 1. Oxygen: Limnology and Oceanography, v. 25, p. 662–671.

Bigham, J.M., Schwertmann, U., Traina, S.J., Winland, R.L., and Wolf, M., 1996, Schwertmannite and the chemical modelling of iron in acid sulphate waters: Geochimica et Cosmochimica Acta, v. 60, p. 2111–2121, doi: 10.1016/0016-7037(96)00091-9.

Bottrell, S.H., and Tranter, M., 2002, Sulphide oxidation under partially anoxic conditions at bed of the Haut d'Arolla, Switzerland: Hydrological Processes, v. 16, p. 2363–2368, doi: 10.1002/hyp.1012.

Carlson, L., Bigham, J., Schwertmann, U., Kyek, A., and Wagner, F., 2002, Scavenging of As from acid mine drainage by schwertmannite: A comparison with synthetic analogues: Environmental Science & Technology, v. 36, p. 1712–1719.

Cornell, R.M., and Schwertmann, U., 2003, The iron oxides: Structure, properties, reactions, occurrences and uses: New York, Wiley, 703 p.

Cuffey, K.M., Conway, H., Gades, A.M., and Raymond, C.F., 1999, Interfacial water in polar glaciers and glacier sliding at −17°C: Geophysical Research Letters, v. 26, p. 751–754, doi: 10.1029/1999GL900096.

Davidson, L.E., Shaw, S., and Benning, L.G., 2008, The kinetics and mechanisms of schwertmannite transformation to goethite and hematite under alkaline conditions: American Mineralogist, v. 93, p. 1326–1337, doi: 10.2138/am.2008.2761.

Gleisner, M., Herbert, R.B., Jr., and Kockum, P.C.F., 2006, Pyrite oxidation by *Acidithiobacillus ferroxidans* at various concentrations of dissolved oxygen: Chemical Geology, v. 225, p. 16–29, doi: 10.1016/j.chemgeo.2005.07.020.

Hubbard, A., Lawson, W., Anderson, B., Hubard, B., and Blatter, H., 2004, Evidence for subglacial ponding across Taylor Glacier, Dry Valleys, Antarctica: Annals of Glaciology, v. 39, p. 79–84.

Hyacinthe, C., and Van Cappellen, P., 2004, An authigenic iron phosphate phase in estuarine sediments: Composition, formation and chemical reactivity: Marine Chemistry, v. 91, p. 227–251, doi: 10.1016/j.marchem.2004.04.006.

Raiswell, R., Canfield, D.E., and Berner, R.A., 1994, A comparison of iron extraction methods for the determination of degree of pyritization and recognition of iron-limited pyrite formation: Chemical Geology, v. 111, p. 101–111, doi: 10.1016/0009-2541(94)90084-1.

Raiswell, R., Tranter, M., Benning, L.G., Siegert, M., De'ath, R., Huybrechts, P., and Payne, T., 2006, Contributions from glacially derived sediment to the global iron (oxyhydr)oxide cycle: Implications for iron delivery to the oceans: Geochimica et Cosmochimica Acta, v. 70, p. 2765–2780, doi: 10.1016/j.gca.2005.12.027.

Raiswell, R., Benning, L.G., Tranter, M., and Tulaczyk, S., 2008, Bioavailable iron in the Southern Ocean: The significance of the iceberg conveyor belt: Geochemical Transactions, v. 9, doi: 10:1186/1467-4866-9-7.

Ruby, C., Aissa, R., Gehin, A., Cortot, J., Abdelmoula, M., and Genin, J.-M., 2006, Green rust synthesis by coprecipitation of Fe^{II}-Fe^{III} ions and mass balance diagram: Comptes Rendus Geoscience, v. 338, p. 420–432.

Schwertmann, U., and Carlson, L., 2005, The pH-dependent transformation of schwertmannite to goethite at 25°C: Clay Minerals, v. 40, p. 63–66, doi: 10.1180/0009855054010155.

Schwertmann, U., and Murad, E., 1983, Effect of pH on the formation of goethite and hematite from ferrihydrite: Clays and Clay Minerals, v. 31, p. 277–284, doi: 10.1346/CCMN.1983.0310405.

Sharp, M., Parkes, J., Cragg, B., Fairchild, I.J., and Lamb, H., 1999, Widespread bacterial populations at glacier beds and their relationship to rock weathering and carbon cycling: Geology, v. 27, p. 107–110, doi: 10.1130/0091-7613(1999)027<0107:WBPAGB>2.3.CO;2.

Tranter, M., Brown, G.H., Raiswell, R., Sharp, M., and Gurnell, A., 1993, A conceptual model of solute acquisition by Alpine glacial meltwaters: Journal of Glaciology, v. 39, p. 571–581.

Tranter, M., Sharp, M., Brown, G.H., Willis, I.C., Hubbard, B.P., Nielsen, M.K., Smart, C.C., Gordon, S., Tulley, M., and Lamb, H.R., 1997, Variability in the chemical composition of in situ subglacial meltwaters: Hydrological Processes, v. 11, p. 59–77, doi: 10.1002/(SICI)1099-1085(199701)11:1<59: AID-HYP403>3.0.CO;2-S.

Waychunas, G.A., Kim, C.S., and Banfield, J.F., 2005, Nanoparticulate iron oxide minerals in soils and sediments: Unique properties and contaminant scavenging mechanisms: Journal of Nanoparticle Research, v. 7, p. 409–433, doi: 10.1007/s11051-005-6931-x.

Williamson, M.A., and Rimstidt, J.D., 1994, The kinetics and electrochemical rate-determining step of aqueous pyrite oxidation: Geochimica et Cosmochimica Acta, v. 58, p. 5443–5454, doi: 10.1016/0016-7037(94)90241-0.

Yee, N., Shaw, S., Benning, L.G., and Nguyen, T.H., 2006, The rate of ferrihydrite transformation to goethite via the Fe(II) pathway: American Mineralogist, v. 91, p. 92–96, doi: 10.2138/am.2006.1860.

Yu, J.Y., Park, M., and Kim, J., 2002, Solubilities of synthetic schwertmannite and ferrihydrite: Geochemical Journal, v. 36, p. 119–132.